

The N-terminal domain of an archaeal multidrug and toxin extrusion (MATE) transporter mediates proton coupling required for prokaryotic drug resistance

**Kevin L. Jagessar<sup>1</sup>, Hassane S. Mchaourab<sup>1</sup> and Derek P. Claxton<sup>1\*</sup>**

<sup>1</sup>From the Department of Molecular Physiology and Biophysics, Vanderbilt University, Nashville, TN 37232, USA

#### Supporting Information

Figure S1. Absorbance of R6G

Figure S2. Cell growth curves in the absence and presence of R6G

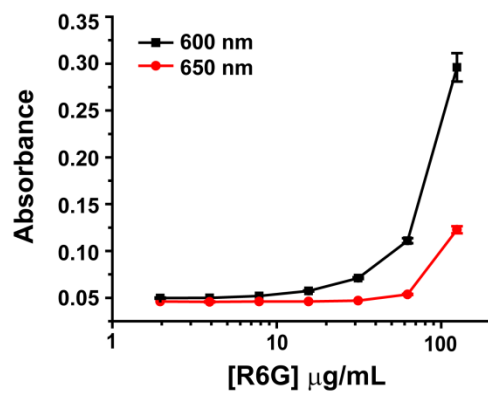
Figure S3. Relative cell growth after induction with 10  $\mu$ M IPTG

Figure S4. Relative cell growth curves in hypersensitive *E. coli* strains

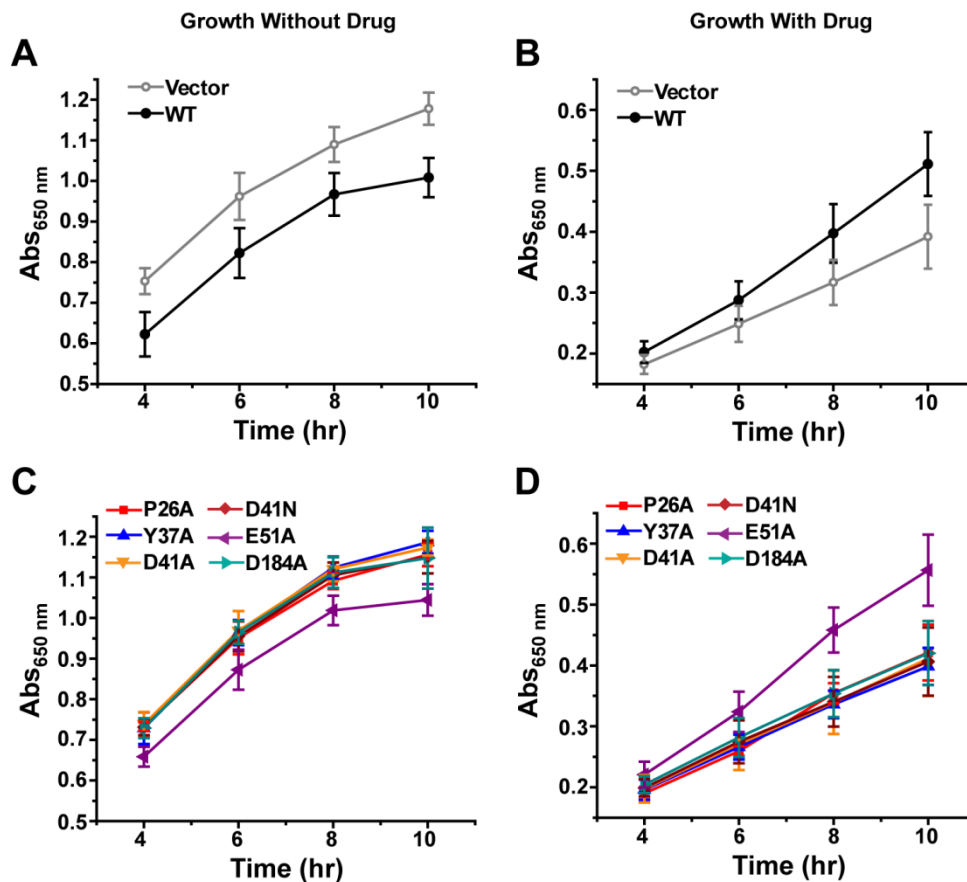
Figure S5. Sequence conservation analysis

Figure S6. PfMATE expression profile

Figure S7. Size exclusion chromatography of purified PfMATE variants



**Figure S1.** Absolute absorbance of R6G at the given wavelengths as a function of R6G concentration on a 96-well plate. Due to relatively high absorbance of R6G at 600 nm, cell growth on the 96-well plate was monitored at 650 nm. Data are shown as the average and standard deviation of triplicate measurements at each drug concentration.



**Figure S2.** Cell growth curves monitored by absorbance at 650 nm of vector and PfMATE variants in the absence and presence of 75  $\mu\text{g}/\text{mL}$  R6G. The growth profiles of cells harboring vector alone and WT PfMATE (panels A and B) are shown separately from the growth profiles of the variants (panels C and D) for clarity. The curves were obtained at 37  $^{\circ}\text{C}$  using the 96-well plate format, and the data shown as the average and standard deviation from  $n=3-6$  experiments. The x-axis indicates the time of growth following a two hr induction period with 1  $\mu\text{M}$  IPTG and dilution of the cells to identical starting Abs<sub>600nm</sub> (0.025) according to the **Experimental Procedures**. (A) Cells expressing WT PfMATE demonstrated reduced growth relative to the vector control in the absence of drug, consistent with the intrinsic challenge of PfMATE expression to cell growth as shown in Fig 1A. (B) However, cells that expressed WT PfMATE showed enhanced growth relative to the vector in the presence of drug. (C and D) Cell growth curves for PfMATE variants in the absence and presence of drug, respectively. The data indicates that functionally-impaired variants (P26A, Y37A, D41A, D41N and D184A) demonstrate similar growth patterns as the vector, whereas E51A is similar to WT. The relative Abs<sub>650nm</sub> reported in Fig 1C and Fig 2B was generated by normalizing the growth in panels (B) and (D) to cell growth in the absence of drug shown in panels (A) and (C).

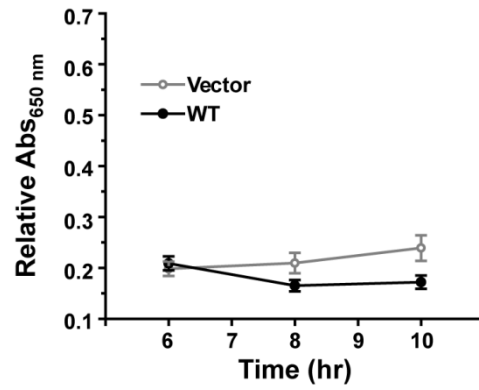


**Figure S3.** Time course of cell growth following induction with 10  $\mu$ M IPTG in medium containing 75  $\mu$ g/mL R6G. Under these conditions, PfMATE-mediated cell survival was not observed relative to the vector control. The y-axis scale is the same as Fig 1C. Data are shown as the average and standard deviation from five experiments and each data point measured in triplicate.

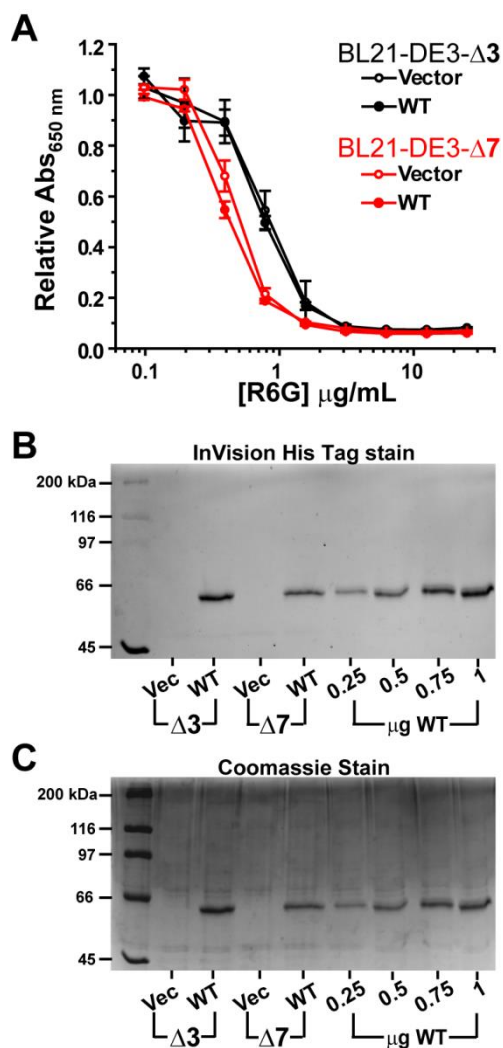


**Figure S4.** Cell growth curves in hypersensitive *E. coli* strains as a function of R6G concentration. (A) These strains are devoid of three ( $\Delta 3$ ) and seven ( $\Delta 7$ ) endogenous multidrug transporters, as described in the main text. Each data point represents the average of two independent experiments. For each experiment, the data was measured in triplicate from separate wells on the plate after 10 hrs at 37 °C. The standard deviation is shown for each data point. Protein expression was confirmed by SDS-PAGE and staining with either InVision His tag stain (B) or Coomassie (C). The last four lanes of each gel image is purified PfMATE WT used as a standard.

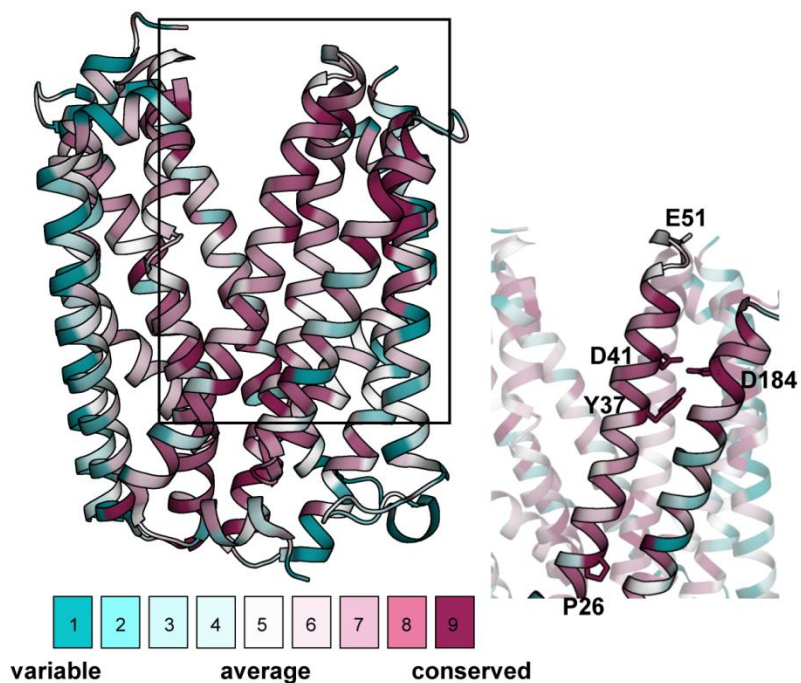


**Figure S5.** Estimation of PfMATE sequence conservation using the ConSurf server. A phylogenetic tree was built from a CLUSTALW multiple sequence alignment of 500 homologous sequences collected from a filtered UNIPROT database (CLEAN-UNIPROT). The homologs were identified by a hidden Markov model (HMMER) search algorithm with a 0.0001 E-value. The relative amino acid conservation scores were calculated using a Bayesian algorithm and mapped onto the PfMATE crystal structure (PDB 3VVN). The conservation scores for each amino acid correspond to the discrete color scale. This analysis shows that the evolutionary rate of P26, Y37, D41 and D184 is slow, and therefore defined as “conserved”. In contrast, E51 is non-conserved.

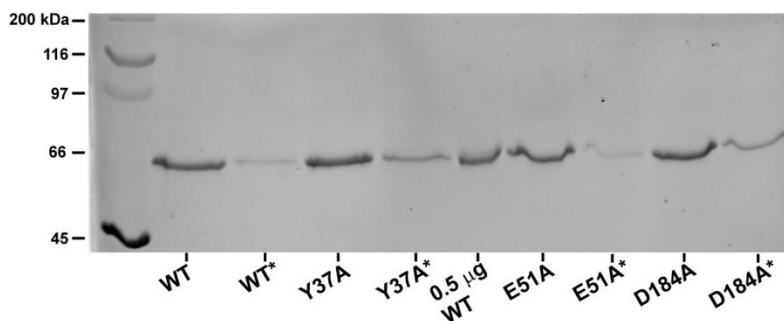


**Figure S6.** PfMATE expression profile for select variants. The presence of WT and variant PfMATE was visualized via SDS-PAGE followed by staining with InVision His tag stain as described in the **Experimental Procedures**. The amount of purified sample loaded into each well was normalized to the membrane mass acquired during processing of culture. For each construct, the first lane shows the amount of PfMATE isolated from culture following induction with 1  $\mu$ M IPTG. The second lane (\*) shows the amount of PfMATE isolated from culture after diluting a fraction of IPTG-induced cells (~50-60 fold) into a similar volume of medium (50% LB broth, 0.1 mg/mL ampicillin), growing the cells at 37  $^{\circ}$ C in the absence of R6G and harvesting at  $Abs_{600nm} = 1.0-1.2$ .

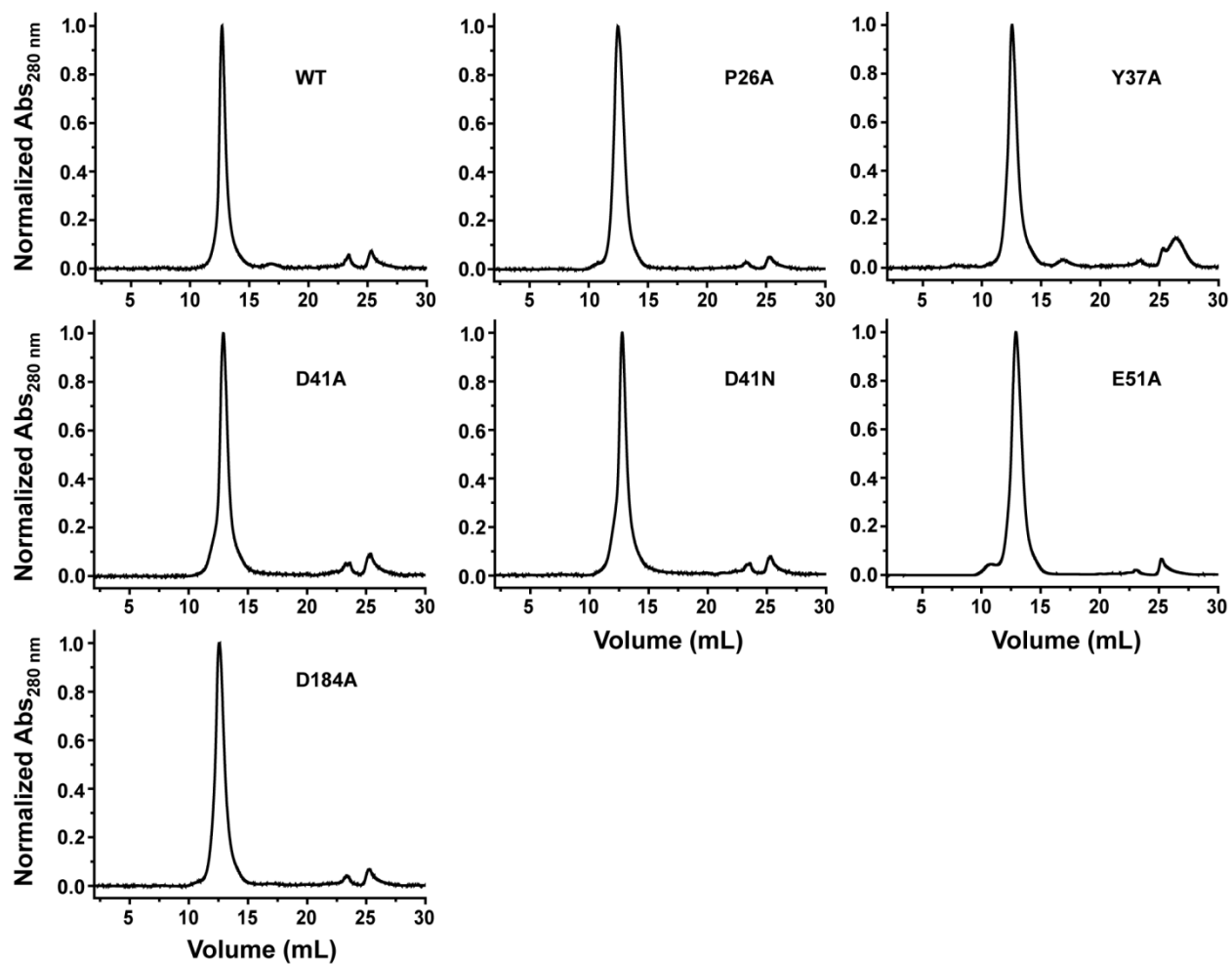


**Figure S7.** Size exclusion chromatography of purified PfMATE variants in  $\beta$ -DDM buffer. Normalized absorbance at 280 nm is shown as a function of elution volume. The chromatograms were acquired at 23 °C on a Superdex200 Increase 10/300 GL column as described in the **Experimental Procedures**.